INTERNATIONAL JOURNAL OF PRECISION ENGINEERING AND MANUFACTURING Vol. 16, No. 7, pp. 1279-1291 JUNE 2015 / 1279
DOI: 10.1007/s12541-015-0167-1 ISSN 2234-7593 (Print) / ISSN 2005-4602 (Online)

Experimental and Numerical Analysis of Breakup Process of Biodiesel Fuel Spray

Jeong-Kuk Yeom[1] and Woo-Sung Jung[1,#]

1 Department of Mechanical Engineering, Dong-A University, 37 Nakdong-daero, 550beon-gil, Saha-gu, Busan, 604-714, South Korea
Corresponding Author / E-mail: jws212@naver.com, TEL: +82-51-200-6983, FAX: +82-51-200-7656

KEYWORDS: Biodiesel, CFD, Common rail, Drag force, Spray, Surface tension

In this study, the experiments and the numerical analysis were performed in order to compare the spray behavior characteristics of diesel and biodiesel, which was intend to compare the spray tip penetration, the spray cone angle and the average droplet diameter. Diesel, palm oil biodiesel, waste cooking oil biodiesel, and soybean oil biodiesel were used for preparing blended fuel, and the ratios of the blended fuel were varied in the BD(Biodiesel)3~BD100 range. The injection pressures (Δp_{inj}) was considered as an experimental variable and was set to 500 bar, 1000 bar, 1500 bar, and 1600 bar by setting injection duration to 500 μs. In the numerical analysis, the initial droplet diameter was set equally with the diameter of hole, and overall numerical analysis condition was based on the experiments. Consequently, it was found that the change of average droplet diameter did not show the large difference according to fuel mixing ratio, and then the spray tip penetration highly depends on the spray pressure rather than the mixing ratio of the fuels.

Manuscript received: July 18, 2014 / Revised: December 3, 2014 / Accepted: February 6, 2015

NOMENCLATURE

C = coefficient
T = temperature
p = pressure
r = radius

SUBSCRIPT

a = ambient
br = breakup
D = drag force
inj = injection
p = particle

1. Introduction

The study on biofuel is actively conducting in many countries beginning that the use of biofuel applicable in the diesel engine has taken its settle as an alternative that can reduce the environment problems. Lim, et al.[1] have conducted the research that investigates for each fuel on the correlation between the constituent elements of the biodiesel and the derived cetane number, and Kim, et al.[2] have researched on the comparison of the fuel characteristics of the existing diesel and the biodiesel by investigating the flame temperature and the soot concentration of the waste cooking oil biodiesel which is one kind of the biodiesel through the two-color method. The biofuels as fuel of an internal combustion engine are largely divided into biodiesel and bioethanol, and among them, the biodiesel is the substitution energy for obtained through chemical reaction such as Esterification[3] as Palm oil biodiesel, Waste cooking oil biodiesel and Soybean oil biodiesel as the fuel used in the diesel engine. In addition the biodiesel absorbs carbon in the production process, and substitutes fossil fuel, and has the advantage such as the ease of blending with existing diesel fuel without special manufacturing process. Because the common-rail engine can inject the fuel with the higher injection pressure than common diesel engine, the combustion is improved by promoting the atomization of the fuel, and also the output and torque can be improved thereby. The diesel engine can significantly not only reduce the emissions such as CO_2, CO and HC through the improved atomization of the fuel, but also the occurrence inhibition of the combustion emissions such as the

noise reduction and the engine power improvement using less fuel is possible. In order to investigate the effects of bio-diesel according to the application of the biodiesel to existing diesel engine, the study analyzing the exhaust gas from the engine that the biodiesel is applied actively is ongoing, and the study on the injection timing control and NOx reduction is the typical study. Lim, et al.[5] the study on the change of the exhaust gas through the injection timing control of fuel has been conducted, and Jeong, et al.[6] has conducted the study on the combustion of biodiesel and the reduction characteristics of the effluent through the pilot injection. To understand the characteristics and the difference of the fuel used in the existing common-rail engine and biodiesel is most necessary in the improvement of biodiesel.[7-9] Eom, et al.[7] have conducted the study on the effect on the spray characteristics and the combustion, and the characteristics of the exhaust gas by setting the concentration of biodiesel and the mixture amount of ethanol as the variables, and Kim, et al.[8] have considered the effect on the spray characteristics by adding biodiesel in existing fuel in the experimental profile. In addition, Park, et al.[9] have conducted the study on the effect on an engine in accordance with the application of biodiesel. Therefore, in this study, after conducting the spray experiments, the numerical analysis method has been established by utilizing the results, and conducted in the direction of comparison and analysis for the change of spray behavior characteristics of existing fuel and biodiesel. As the study of numerical analysis on diesel spray Wang, et al.[10] connected the analysis of the internal flow of the nozzle using ELSA (Eulerian-lagrangian spray and atomization) model with the external flow, and obtained SMD (Sauter mean diameter), AMD (Arithmetic mean diameter) by the numerical method, and then they have studied on the numerical analytical application for the spray behavior by comparing with the derived value by the experiments. There are Kato, et al.,[11] Postrioti, et al.[12] as the typical study on the external flow analysis of a nozzle, and Kato, et al.[11] have studied for the characteristics of the combustion and the exhaust gas by using two kinds of common-rail type injector that the injection velocity and the internal structure are different each other, and Postrioti, et al.[12] have compared for the degree that the spray behavior is changed after progressing the experiments and the numerical analysis by applying the high pressure condition to the common-rail type. In addition, as the study on the optimization of the nozzle, Kurimoto, et al.[13] have investigated the change of the spray penetration and the spray cone angle according to the nozzle shape through the study that compares the optimization method and the spray behavior characteristics of the experiments and numerical value. This is a preliminary study of biodiesel spray behavior characteristics by using experiment and numerical analysis. The objective of this study is to suggest spray's micro-behavior part quantitatively. In this study, ANSYS-CFX which is CFD commercial program was used to reproduce the change of spray penetration and average droplet diameter according to the change of fuel mixing ratio, and then have conducted the numerical analysis through the experiments, and each conditions were equally set with the experiments.

2. Experimental Method

Fig. 1 is the schematic diagram of the experimental equipment

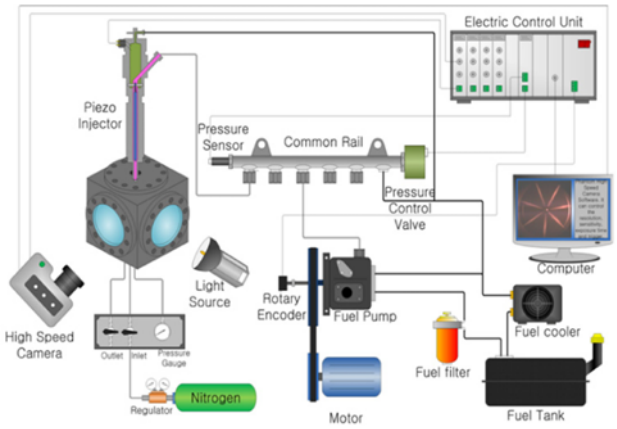

Fig. 1 Schematic diagram of experimental apparatus[4]

Table 1 Experimental conditions

Injection nozzle	7 holes Bosch nozzle
	Hole diameter : 0.119 [mm]
Ambient gas	Air
Ambient temperature (T_a)	298 [K]
Ambient pressure (p_a)	1.01 [bar]
Injection pressure (p_{inj})	500, 1000, 1500, 1600 [bar]
Injection duration (t_{inj})	500 [μs]
Injection fuel	- Diesel only (BD2) - Diesel + Palm oil - Diesel + Waste cooking oil - Diesel + Soybean oil

which consists of the common-rail system and the multihole injector and a high-speed cameras controlled by ECU used in this experiment. The common-rail system containing the common-rail, fuel filter and fuel pump was consists of the pride U-engine genuine goods. The ECU used in the experiment is a universal ECU (SCR-TDA8000, SmarTec) manufactured for experiment, and it consists of four inject drivers which control the fuel injection time and the injection pressure control and the high-speed camera's shooting trigger signal. The fuel injection pressure of the common-rail is the range from 300 bar to 1600 bar, and the fuel injection duration of the injector is possible to set from 100 μs to 4000 μs, and the injector used in the experiment is multiholes (7 holes injector, Bosch) which is a commercial nozzle. The high-speed camera (Micro-4C, Phantom) and two 1kW halogen lighting were used to get the spray images according to the fluctuation of the experimental conditions. The fuel filter was replaced along with the fuel to prevent the contamination due to other fuel when replacing the injection fuel. In this experiment, the ambient condition is the atmospheric pressure at room temperature (1 bar, 298 K), and the injection duration was fixed at 500 μs. Three kinds of fuels (palm oil biodiesel, waste cooking oil biodiesel and soybean oil biodiesel) were used for manufacturing the blended fuel, and the volume ratio BD2 (Diesel only), BD3, BD5, BD20, BD30, BD50 and BD100 varying the mixing ratio of diesel and biodiesel fuel were used as experimental parameters, and the injection pressure was used in this experiment setting as 500 bar, 1000 bar, 1500 bar and 1600 bar for each fuel. The images taken from the front of the nozzle tip and the images taken from the side were acquired as optical

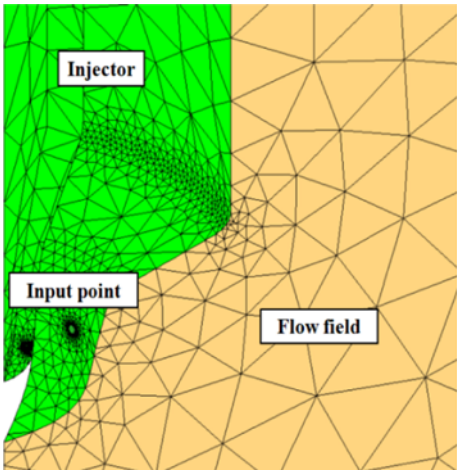

Fig. 2 Expanded mesh of nozzle and flow area

images, and the spray penetration and the spray cone angle were measured on the side image, and the experimental conditions are shown in Table 1.

3. Numerical Analysis Method

ANSYS-CFX was used as the numerical analysis method in this study. The finite volume method is basically used in CFX, unlikely the finite element method generally used to analyze making a connection between the fluid flow analysis and the structural analysis. Usually, the finite volume method is applied to indicate the flow of fluid and heat, and it is the method that obtains the approximate solution subdividing into the finite volumes by the approximate analysis technique based on Euler description.

3.1 Modeling for shape and grid of a nozzle for numerical analysis

The modeling for the shape of the material used in the experiment and the flow field should be preceded to implement more neighboring result to experimental result by using the numerical analysis. Thus, in this paper, first, the experiment was conducted, and the modeling of the flow field was performed based on the fluid area and prior conducted experiment after measuring the internal size by cutting in half the commercial nozzle used in the experiment, and the results are shown in Fig. 2.

Fig. 2 shows the image that magnifies the input point of the entire models having the grid which the node number is about 2.3 million pieces and the element number is about 13 million pieces by setting the minimum size of the element as 2.16×10^{-4}, and by setting the maximum size as 1.5×10^{-3}. The shape of the grid was a tetrahedrons type, and the patch conforming algorithm was used. The reason is because it is possible to shorten the time of this numerical analysis because the surface creates the element mesh in the edges or faces prior to volume in contrast with the patch independent algorithm.

3.2 Boundary condition

The initial value in the default setting of numerical analysis was set based on the experimental results, and the variable assumed that would

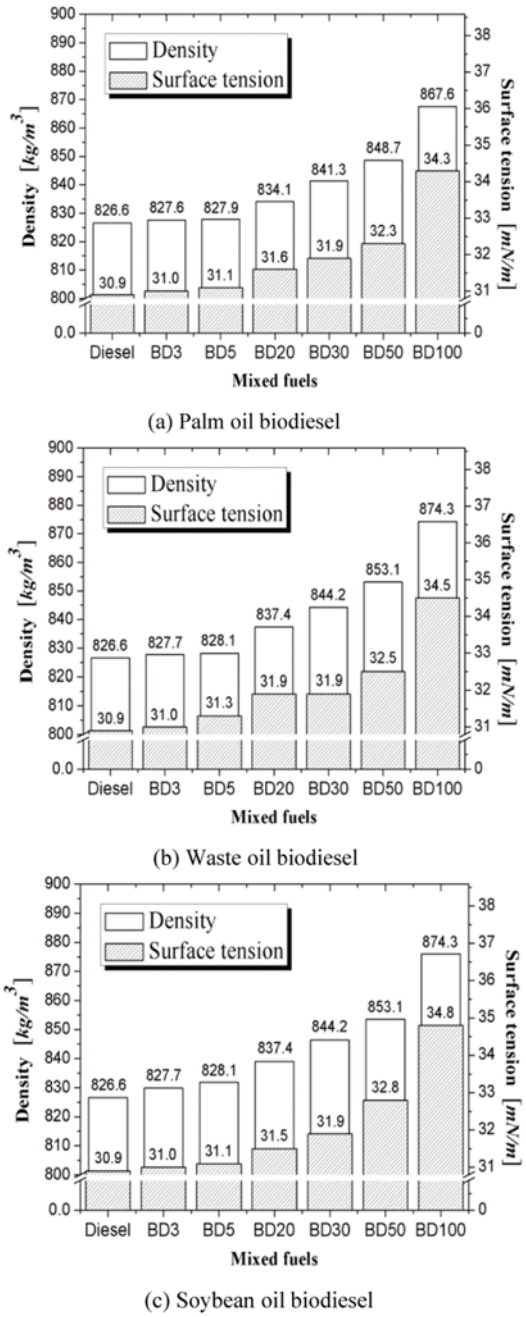

Fig. 3 Variation of density and surface tension for each fuel mixing ratio

have the greatest impact on the numerical analysis among the setting values was determined as the hole diameter and spray cone angle. Because this numerical analysis study was progressed changing the fuel and the injection pressure for the same nozzle, the hole diameter and the internal shape is the same as the experimental condition. In addition, after making sure that there are no great changes as about 6° at 500 μs after starting the injection regardless of the fuel used through the experiments, that value was used the setting values of the numerical analysis for the spray cone angle, and the surface tension and density among other initial setting values necessary for the numerical analysis were directly measure through the experiment, and the results were shown in Fig. 3. Because this experiment was conducted at room

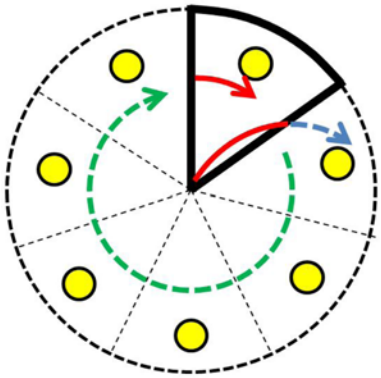

Fig. 4 Boundary condition explanation about domain interface

temperature and under atmospheric pressure (1 bar, 298 K), the flow field region was set as the opening condition that the inflowing and outgoing are free. On the other hand, unlike the typical fluid analysis, because the analysis of spray droplets require the considerable mesh number, 7 holes injector was divided into 1/7 in meeting to the purpose called the time-saving, and the condition was given as the area that the points of contact in the sides can interchange the effect each other, and the condition is the same as shown in Fig. 4. In addition, SST (Shear stress transport) model was used as the turbulence model. The SST model, unlike the k-ε model which is a general-purpose turbulence model, includes the shear transport equation, and has the features providing high accuracy. It is important to set up the drag force in order to observe the movement and the breakup of droplets in the spray-related numerical analysis. Jeon et al.[14] have conducted the study on the spray tip penetration and the breakup in the condition that the ambient pressure and the density were changed. The liquid which the breakup is progressed has not high Reynolds number due to the breakup. As a result, in order to calculate the drag force, the Schiller-Naumann model determined as the model that is the best suited among a variety of drag force models, was applied in this study. This model is generally used frequently for the analysis of the small solid particles, but it is the model applicable for the flow of the fluid with the small droplets. In the Schiller-Naumann model, the expression that determines the drag coefficient is expressed as Eq. (1). The applicable fluid is the two phase flow of the biodiesel (BD2, BD3, BD5, BD20, BD30, BD50 and BD100) that is defined the fluid having the breakup with the air and air defined as the continuum under atmospheric pressure at room temperature. The study was set to overall the transient, and was set so that the spray was made up to 500 μs that was the injection duration, and was calculated up to 700 μs also to observe the spray behavior characteristics after the injection end. The time interval Δt (Time step) calculating was set as 4 μs, and the droplet diameter at the initial of injection was set as the same about 0.12 mm as the hole diameter.

$$C_D = \begin{cases} \frac{24}{Re_p}(1+0.15Re_p^{0.687}) & if \quad Re_p \le 800 \\ 0.44 & if \quad Re_p > 800 \end{cases} \tag{1}$$

In this equation, C_D means the drag coefficient, and Re_p means the Reynolds number of a droplet.

Table 2 CAB breakup model constants and default values

Coefficient	Value	Means
k_1	0.05	CAB Bag Breakup Factor
We_t	80	Critical Weber Number for stripping Break up
We_{t2}	350	Critical Weber Number for Catastrophic Break up
C_k	8	Restoring Force Coefficient
C_b	0.5	Critical Amplitude Coefficient
C_f	1/3	External Force Coefficient

3.3 Breakup model

What that derive a more reliable calculation by setting the breakup model in the numerical analysis is particularly important in the spray analysis. As a study on the breakup model, Ko, et al.[15] have conducted the research that finds a suitable model through the change of the breakup model and the drag force model. In this paper, the numerical analysis was conducted by applying CAB (Cascade atomization and breakup) model as the breakup model. CAB model is the developed model of ETAB (Enhanced Taylor analogy breakup) model as a kind of secondary breakup model, and the equation the same as Eq. (2) is used to determine the radius of a child droplet, $r_{p,Child}$ using the radius of a parent droplet, $r_{p,Parent}$, and t means the time in this equation. Eq. (3) is the formula used to determine stripping breakup coefficient k_2. Where, the stripping breakup means the breakup that small droplets are separated from larger droplets, and the default coefficient value of the initial setting in Eq. (4) used to define C_k, C_b and C_f and the breakup coefficient K_{br} and k_3 used in Eq. (3) are the same as Table 2.

$$\frac{r_{p,Child}}{r_{p,Parent}} = e^{K_{br}t} \tag{2}$$

$$k_2 = k_1 \frac{\sqrt{1-\frac{1}{2}\left(\frac{C_k C_b}{C_f We_t}\right)}}{\operatorname{acos}\left(1-\frac{C_k C_b}{C_f We_t}\right)} \tag{3}$$

$$K_{br} = \begin{cases} k_1 w \\ k_2 w\sqrt{We} \\ k_3 w We^{0.75} \end{cases} \qquad k_3 = \frac{k_2}{We_{t2}^{0.25}} \tag{4}$$

4. Results and Discussion

In this paper, the authors intended to propose the numerical analysis of the biodiesel spray through the comparison the experimental results and the results of the numerical analysis, and the injection pressure of injector and biodiesel mixing ratio were set as the experimental variables, and the effect on the spray penetration and the spray cone angle which are macroscopic spray behavior characteristics was observed. The spray cone angle of the initial input condition of the numerical analysis was measured by using the side image obtained through a high-speed camera, and the density and the surface tension that are the properties of the injection fuel applied were in-advance measured, and by applying the results to the calculation, this paper was conducted in the direction to establish the suitable interpretive method

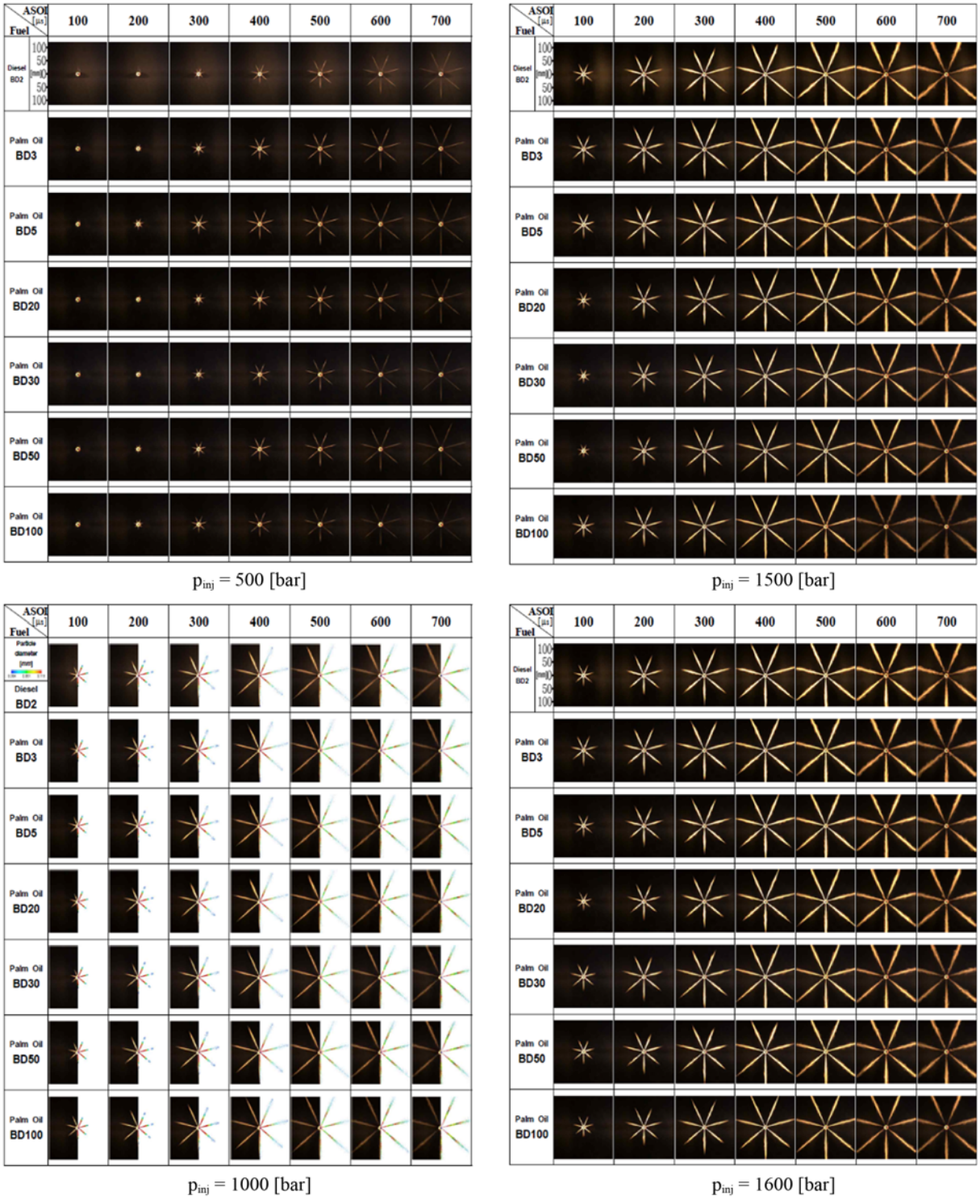

Fig. 5 Image of spray behavior for palm oil biodiesel with injection pressure (front view)

through the comparison between the experimental results and the numerical analysis results.

4.1 Consideration for spray behavior characteristics using experiments

The observation of the front view and the side view of the spray behavior in order to improve the reliability was performed. Also, it is necessary to obtain suitable boundary condition for numerical analysis.

Figs. 5, 6, and 7 show the front view images taken by a high-speed camera at the time interval of 100 μs and under the injection pressure of 500 bar, 1500 bar, and 1600 bar for each fuel, and they also show the comparison of experimental analysis results on the right and numerical analysis results on the left for the injection pressure, p_{inj}=1000 bar. Each fuel shows that the spray tip penetration is increased as the injection pressure is increased, and it can be seen from the overall trend, that the fuel droplets are distributed a lot in the center in comparison with the

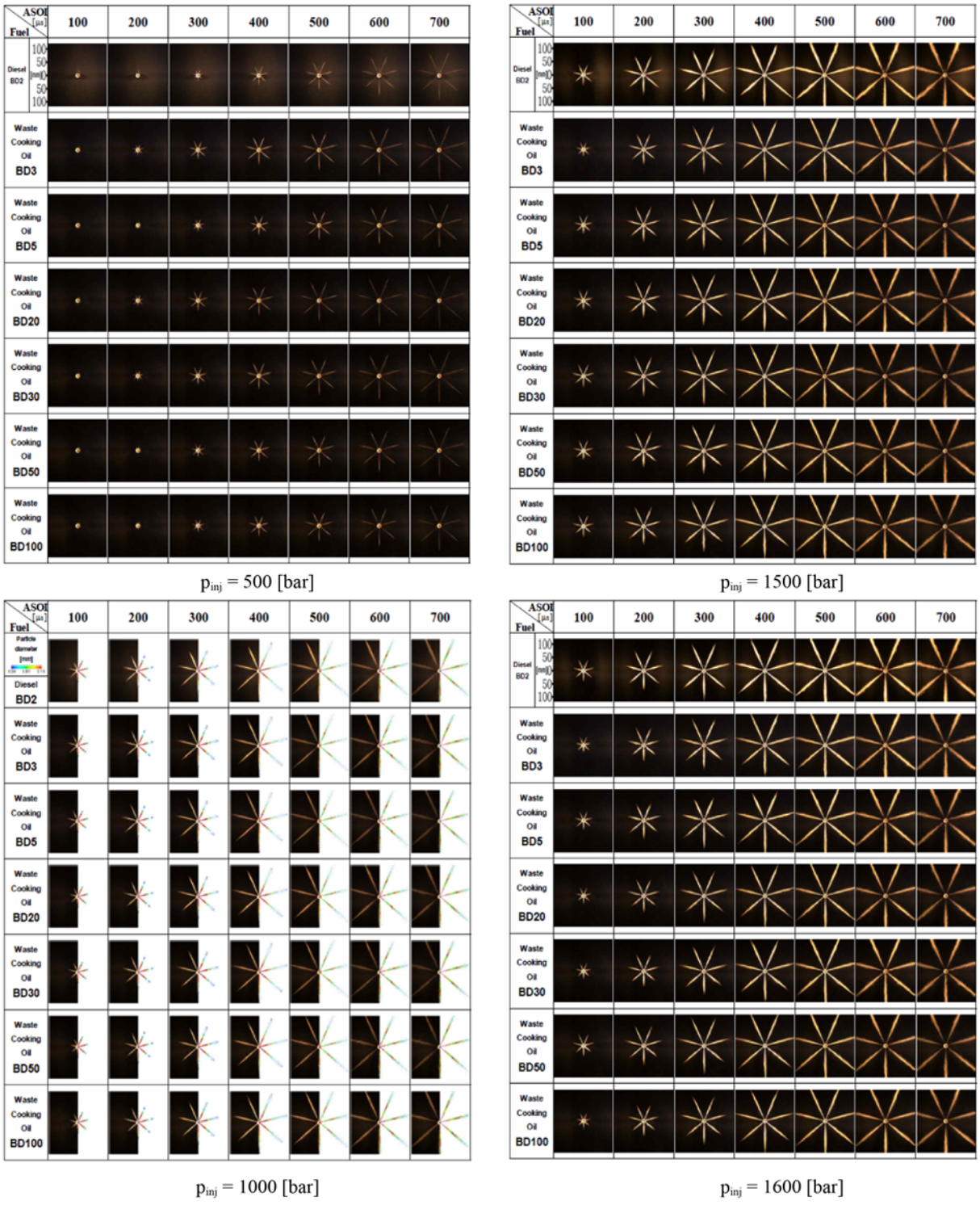

Fig. 6 Image of spray behavior for waste cooking oil biodiesel with injection pressure (front view)

surface portion, which is the general behavioral aspect of the full cone spray. Also it can be seen from the Figures that the macroscopic spray behavior characteristics of the spray tip penetration shows good agreement between the experimental and the numerical analysis values.

Figs. 8, 9 and 10 are the side view images for each fuel and pressure. The spray tip penetration and the spray cone angle were measured by the same method as in Fig. 11 based on these images. As a result, the spray tip penetration was derived as shown in Fig. 12 under the p_{inj}=1000 bar condition that can compare the experimental results and the numerical analysis, and unlike the initial prediction said that the spray behavior characteristics will be changed according to the basic properties changes of fuel, the spray behavior characteristics of biodiesel macroscopically shows a little change for the properties of fuel, whereas the aspects that the behavior characteristics that in the case of high-pressure injection, the spray tip penetration is increased than the case of low-pressure injection is the same as the previous

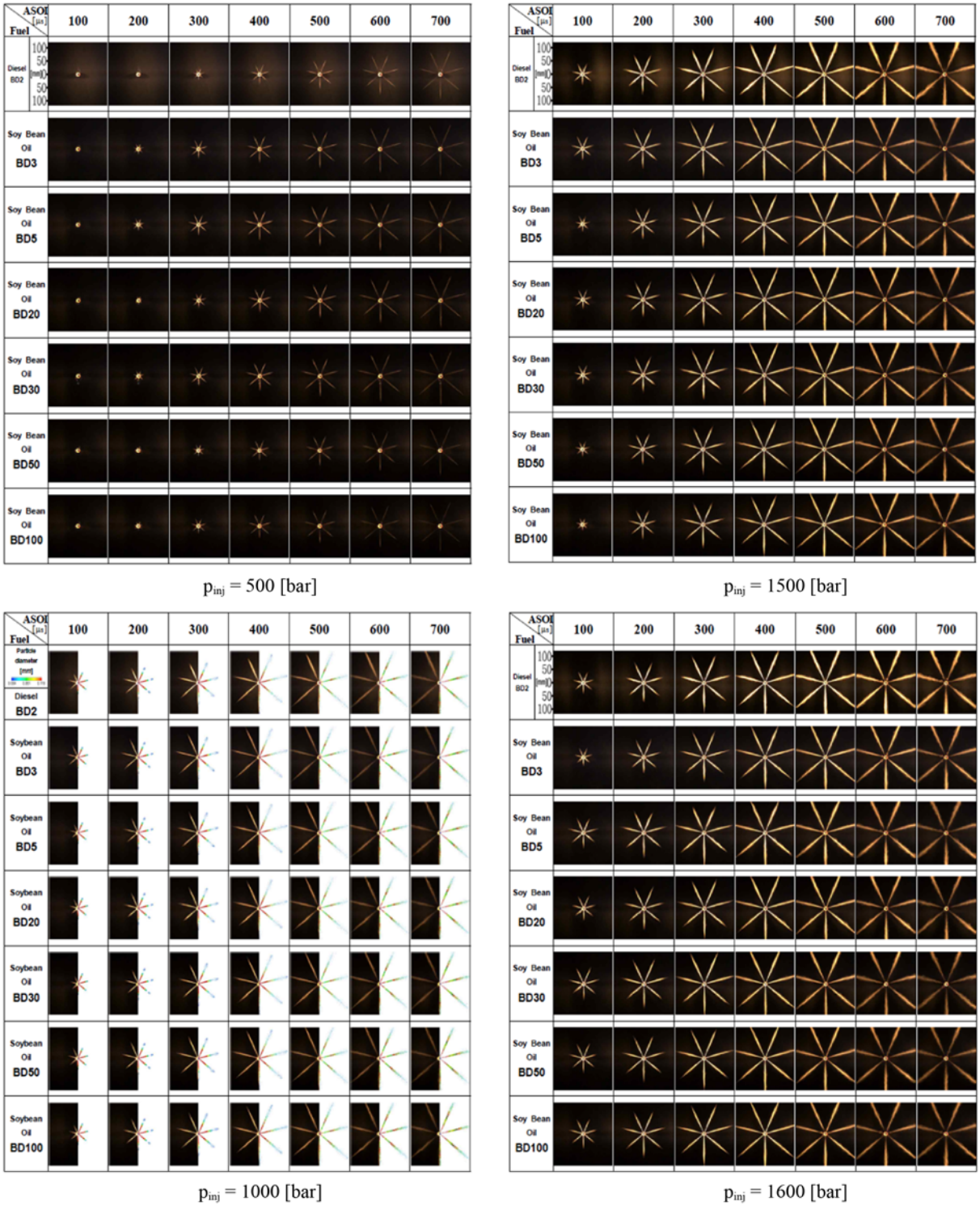

Fig. 7 Image of spray behavior for soybean oil biodiesel with injection pressure (front view)

research results.[16] It is considered that because the properties difference of the viscosity and the surface tension between the biodiesel and existing diesel in the high-pressure injection condition of the common-rail system does not appreciably affect the spray behavior characteristics. In addition, examining the change of the spray tip penetration derived by applying the numerical analysis in Fig. 12, it can be confirmed that approximate to length experimentally measured, and also it can be confirmed that do not largely dependent to the properties of fuel in the same manner as the experimental results, and it can be seen that does not have a large error compared to the experimental values when implementing the spray behavior applying the experimental boundary condition. As a result, in both cases of the experiment and the numerical analysis, the spray behavior characteristics were influenced more dominant by the injection pressure than the fuel mixing ratio, and the spray cone angle was not seen large different every fuel.

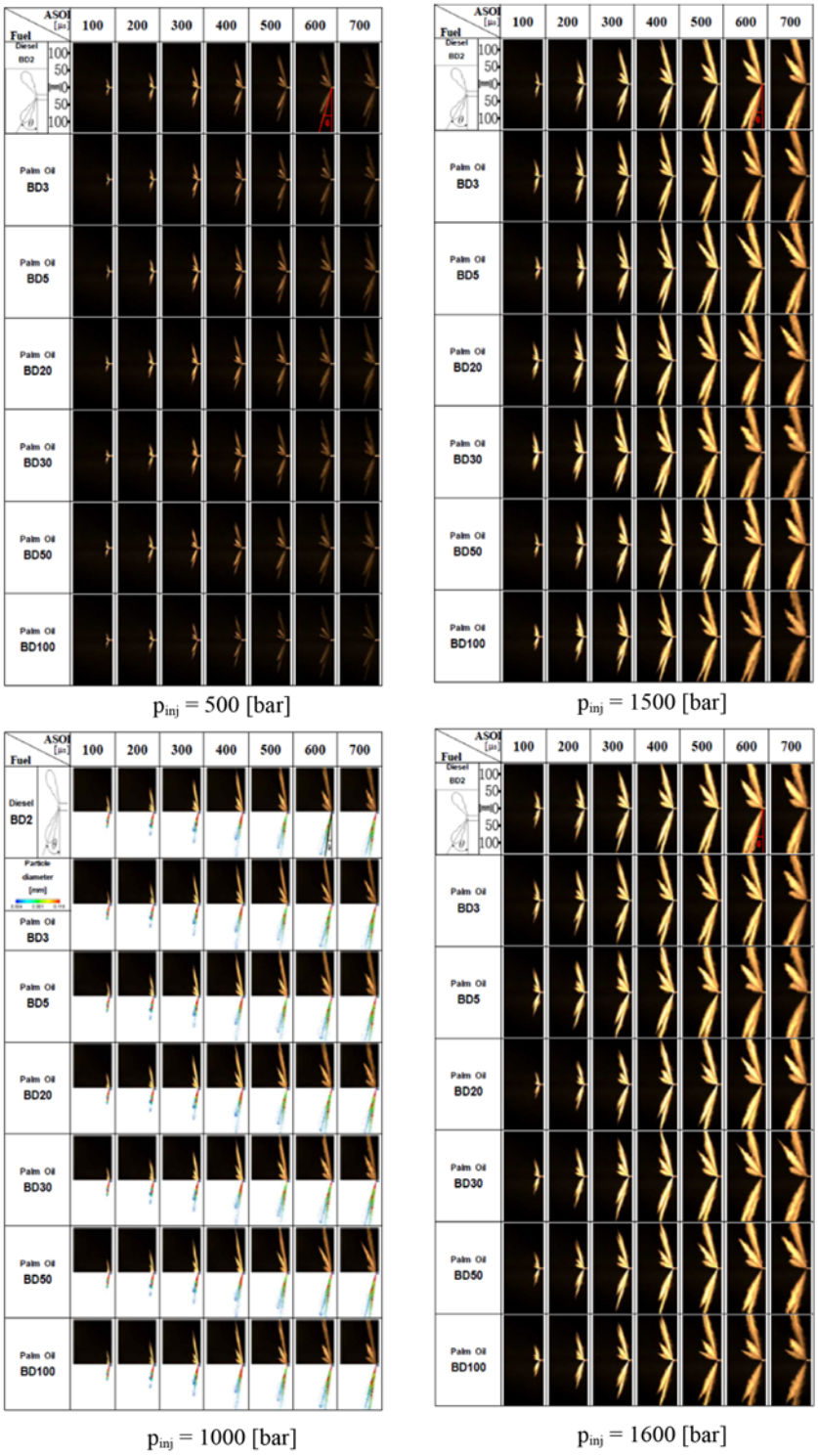

Fig. 8 Image of spray behavior for palm oil biodiesel with injection pressure (side view)

4.2 Consideration for spray behavior characteristics using numerical analysis

Figs. 5-10 showed by comparing the results of the experiment and numerical analysis for the results of 1000 bar as the representative value among the injection pressure of each fuel in order to compare the results obtained through the experiment and the numerical analysis. The initial droplet diameter for numerical analysis was the same as the hole diameter of injector nozzle. As shown in Fig. 11 which is a schematic diagram of the spray characteristics, the area that fuel can be macroscopically observed and the area that can be observed on the numerical analysis because fuel was atomized through breakup due to the resistance of the fuel and the ambient gas can be confirmed. It is considered that the reason is because the droplets broken up cannot be confirmed due to lack of spatial resolution of high-speed camera used in the experiment. Kurimoto's study[13] is similar to this, and Kurimoto et al.[13] have compared both results by carrying out the experiment and

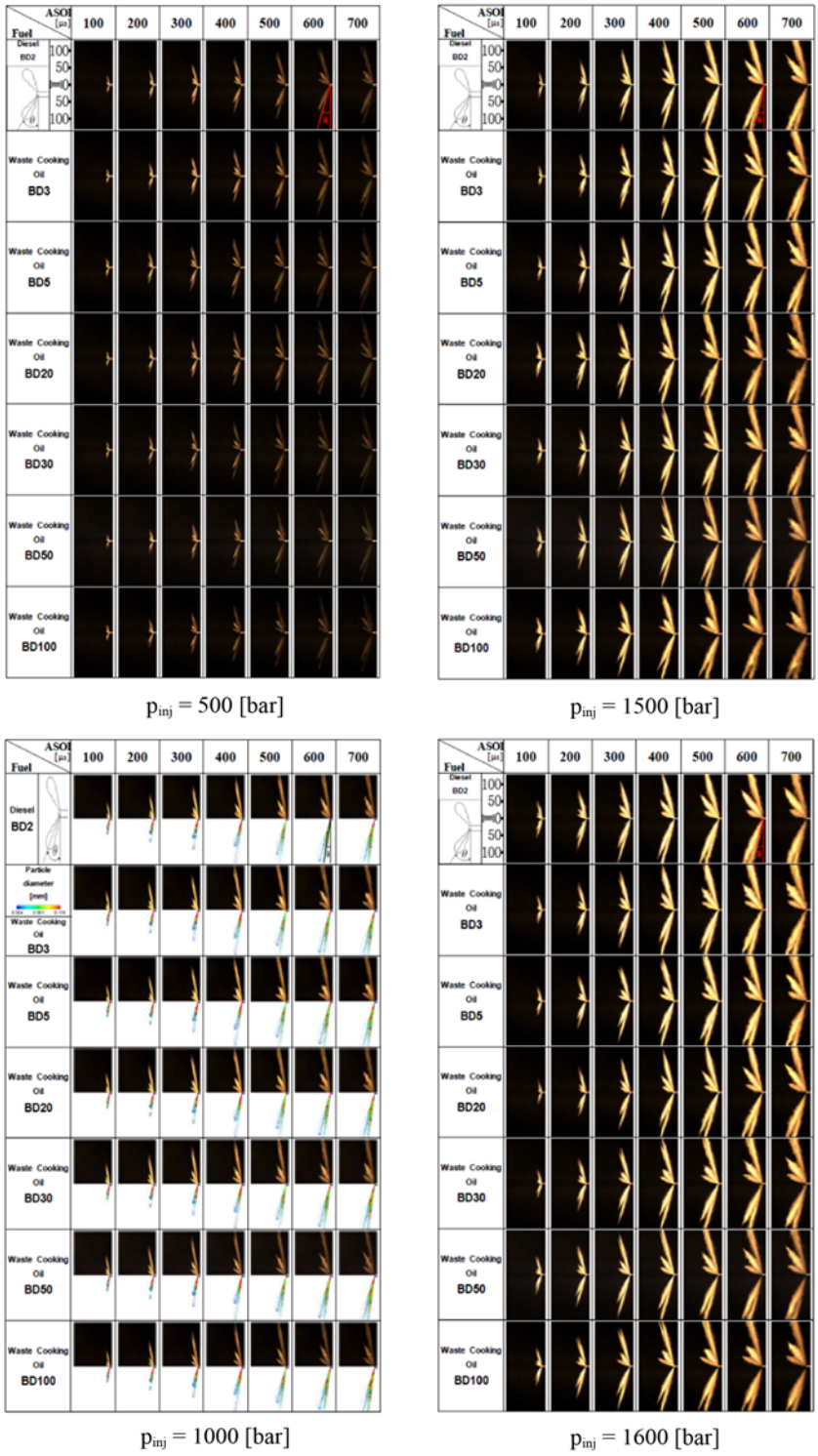

Fig. 9 Image of spray behavior for waste cooking oil biodiesel with injection pressure (side view)

the numerical analysis, and they have considered the reason by grasping the case that the difference of two kinds of the spray characteristics was occurred. It is considered that the setting of Schiller-Naumann model which is the drag force model applied to small fluid droplets in this paper among the conditions applied to the numerical analysis, has a decisive effect on them. Thus, in this study, the change of the spray behavior characteristics according to the change of the drag force in the diesel injection was shown in Fig. 13. These models were divided into two types of the Schiller-Naumann model used in this numerical analysis and the specified drag coefficient set to a constant value. The specified drag coefficient was again classified into 5 and 10. In the Schiller-Naumann model, the drag force value depends on the Reynolds number in low Reynolds number, but if it reaches to more than 800, it has value of 0.44. As a result comparing each condition of Fig. 13, overall the more the value of drag coefficient is increased, the less the breakup becomes reduced by the atmospheric

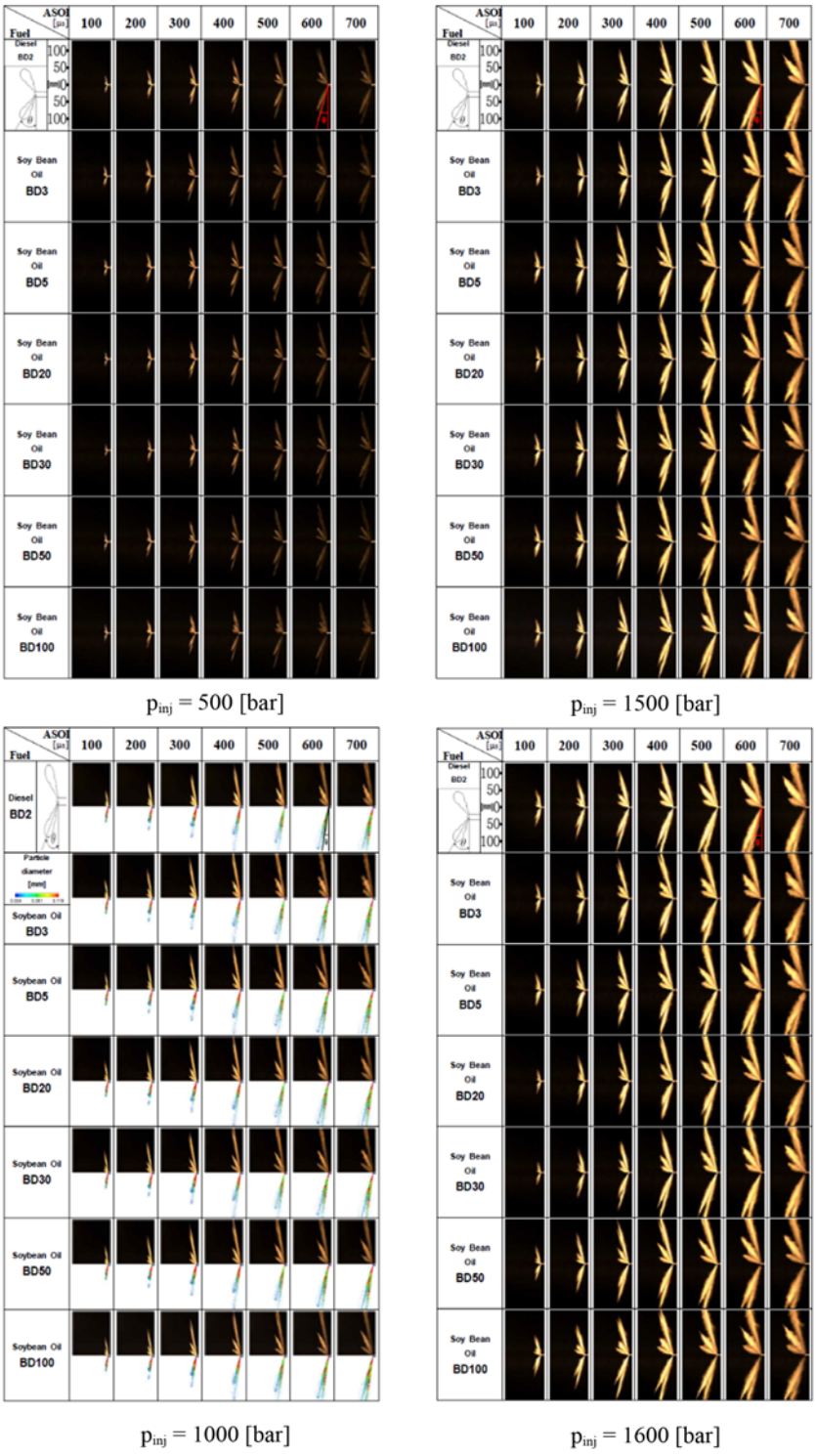

Fig. 10 Image of spray behavior for soybean oil biodiesel with injection pressure (side view)

gas and the size of droplet can see to increase, and it has obtained the conclusion that if the drag coefficient is increased to more than a certain value, the result different from the original spray behavior characteristics is occurred. In Fig. 14, the occurrence of the breakup by the friction in the surface portion than the center of spray caused by the resistance atmosphere gas is more active. As a result, the fuel droplets are identically distributed much more in the center than the surface portion of the fuel spray as the above-mentioned. For this reason, as shown in Fig. 13, the area that the droplets are concentrated is clear in the Schiller-Naumann model than the others, and it can be seen that the region is closed to the experimental results.

Fig. 15 shows the graph comparing the average droplet diameter in time interval of 100 μs from 0 to 700 μs through the frequency of droplet. It can see through Fig. 15 that the average droplet diameter becomes relatively large as the drag coefficient is increased. As the results macroscopically observing the spray behavior characteristics

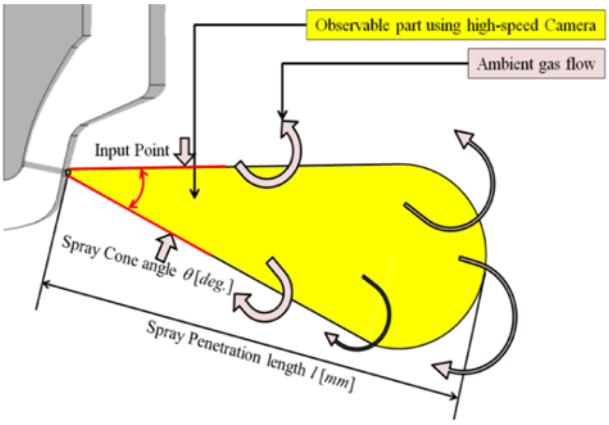

Fig. 11 Comparison of the experimental and numerical particle distribution

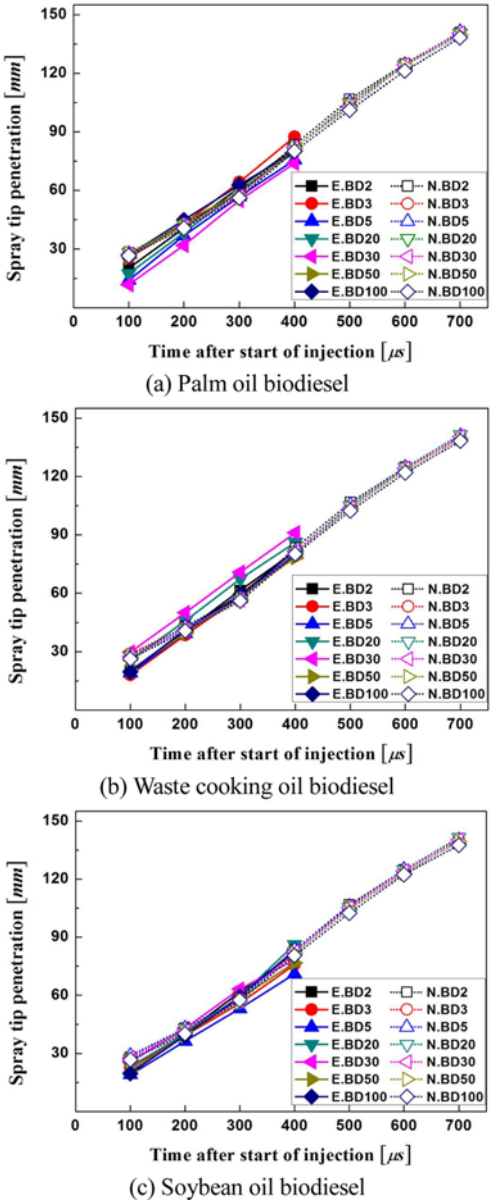

Fig. 12 Comparison of spray penetration about each fuel mixing ratio in p_{inj}=1000 bar condition

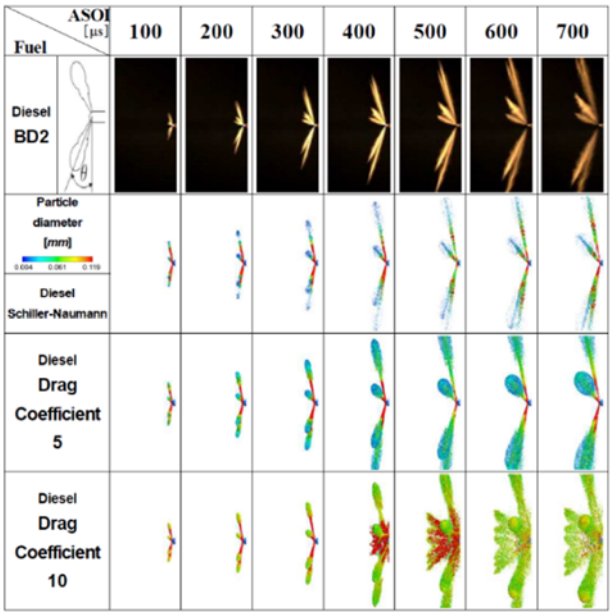

Fig. 13 Images of spray behavior for drag force in p_{inj} = 1000 bar condition

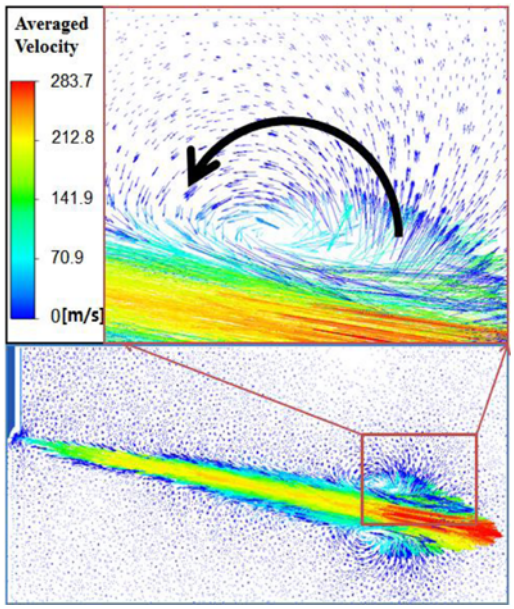

Fig. 14 Averaged velocity vector of injected fuel

according to overall fuel mixing ratio in order to compare the spray behavior characteristics in terms of the numerical analysis based on these drag model condition, there were no significant change. In order to observe in the microscopic respect, the average value obtained using diameter and number of the entire droplets according to each over time in the same manner previously conducting is shown in Fig. 16 according to the fuel mixing ratio. In the front and side view images taken with the camera, like that the spray behavior did not show any macroscopic change, the average diameter value also almost was no change. The spray behavior characteristics shows slight differences depending on the fuel air ratio, but it was judged that it is influenced

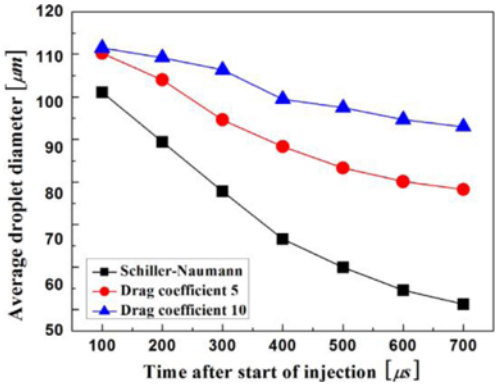

Fig. 15 Variation of average droplet diameter with drag force

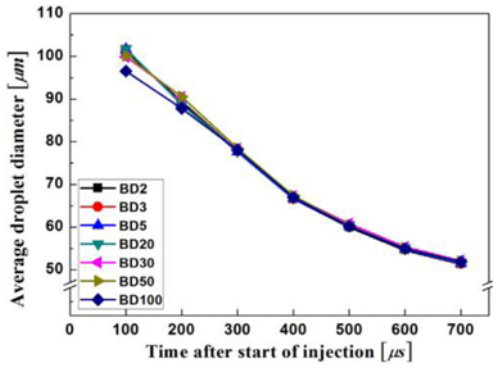

(a) Palm oil biodiesel

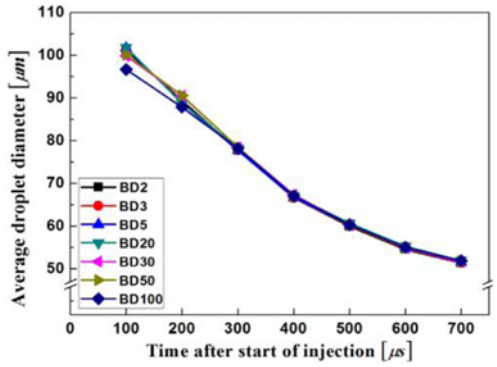

(b) Waste cooking oil biodiesel

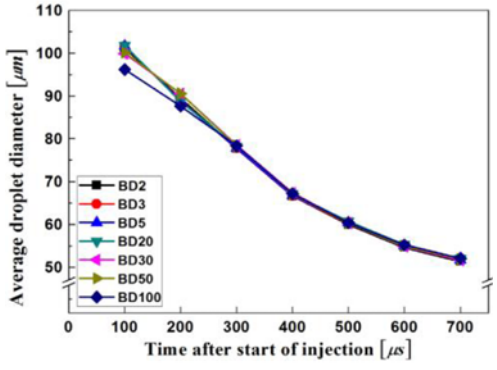

(c) Soybean oil biodiesel

Fig. 16 Average particle diameter for each fuel mixing ratio

more dominant by the injection pressure.

5. Conclusions

In this study, the macroscopic behavior characteristics of the diesel spray according to the mixing ratio of diesel and biodiesel (BD2, BD3, BD5, BD20, BD50 and BD100) and the change of injection pressure were investigated. The injection pressure p_{inj}=1000 bar was selected as the representative value of setting pressures. The results are compared with the numerical analysis results obtained by using commercial software. The conclusions made are listed below.

(1) By observing the spray behavior according to the change in the injection pressure and the fuel mixing ratio, it is found that the fuel spray is influenced dominantly by injection pressure which is in agreement with the existing research results. The spray behavior change due to the change in properties such as the density and surface tension and also the change of biodiesel mixing ratio was not significant because the properties of biodiesel fuel after esterification reaction are very similar to diesel.

(2) In this paper, in order to select the appropriate drag model, Schiller-Naumann model and specified drag coefficients (5, 10) were applied. Consequently, it was confirmed that Schiller-Naumann model is the most suitable for the reproduction of the spray behavior. In addition, it was confirmed that by applying the CAB model as the breakup model, the spray tip penetration measured through the experiment is comparable to the spray tip penetration obtained through the numerical analysis.

(3) In this study, the diameter and the frequency of the entire droplets were calculated through the numerical analysis. Consequently, the rate of change in the average droplet diameter was confirmed by using the numerical results for each fuel mixing ratio.

ACKNOWLEDGEMENT

This research was supported by Basic Science Research Program through the National Research Foundation of Korea (NRF) funded by the Ministry of Education, Science and Technology (NRF-2013R1A1 A2011842).

REFERENCES

1. Lim, Y. K., Park, S. R., Kim, J. R., Yim, E. S., and Jung, C. S., "The Study of Correlation between Biodiesel Components and Derived Cetane Number," Transactions of the Korean Society of Automotive Engineers, Vol. 19, No. 3, pp. 122-129, 2011.

2. Kim, M. S. and Kang, H. Y., "Measurement of Soot and Temperature on Bio Diesel Flame by Two-Color Method," Journal of the Korea Society For Power System Engineering, Vol. 16, No. 4, pp. 5-11, 2012.

3. No, S. Y., "Bioenergy Engineering," ABCNURI, Chungbuk National University, pp. 47-60, 2009.

4. Yeom, J. K., "Basic Experimental Study on the Application of Biofuel to a Diesel Engine," Transactions of the KSME (B), Vol. 35, No. 11,

pp. 1163-1168, 2011.

5. Lim, J. K. and Cho, S. G., "Effects of Fuel Injection Timing on Exhaust Emissions Characteristics of Biodiesel Blend Oil in Diesel Engine," Journal of the Korean Society of Marine Engineering, Vol. 36, No. 5, pp. 603-608, 2012.
6. Jeong, K. S., Lee, D. G., Roh, H. G., and Lee, C. S., "Effect of Pilot Injection on Combustion and Exhaust Emissions Characteristics in a Biodiesel Fueled Diesel Engine," Journal of the Korean Society of Combustion, Vol. 16, No. 4, pp. 1-7, 2011.
7. Eom, D. S., Choi, Y. S., Cho, Y. S., and Lee, S. W., "Spray and Combustion Characteristics of Biodiesel-Ethanol Blending Fuel," Transactions of the KSME (B), Vol. 17, No. 3, pp. 1-7, 2009.
8. Kim, J. D., Ainull, G., Song, K. K., Jung, J. Y., and Kim, H. G., "An Experimental Study on Spray Characteristics of Diesel and Bio-diesel Fuel," Journal of the Korean Society of Marine Engineering, Vol. 35, No. 1, pp. 53-59, 2012.
9. Park, K. H., Kim, J. Y., Kim, C. J., Ko, J. H., and Park, H. I., "The Effect of Bio-diesel Fuel on Industrial Diesel Engine," Journal of the Korean Society of Marine Engineering,Vol. 36, No. 1, pp. 111-116, 2012.
10. Wang, Y., Lee, W. G., Reitz, R. D., and Diwakar, R., "Numerical Simulation of Diesel Sprays using an Eulerian-Lagrangian Spray and Atomization (ELSA) Model Coupled with Nozzle Flow," SAE Technical Paper No. 2011-01-0386, 2011.
11. Kato, A., Matsuura, K., Hakozaki, Y., Suzuki, P., Haraguchi, S., et al., "Influence of a Fast Injection Rate Common Rail Injector for the Spray and Combustion Characteristics of Diesel Engine," SAE Technical Paper No. 2011-01-0687, 2011.
12. Postrioti, L., Battistoni, M., Ungaro, C., and Mariani, A., "Analysis of Diesel Spray Momentum Flux Spatial Distribution," SAE Technical Paper No. 2011-01-0684, 2011.
13. Kurimoto, N., Suzuki, M., Yoshino, M., and Nishijima, Y., "Response Surface Modeling of Diesel Spray Parameterized by Geometries Inside of Nozzle," SAE Technical Paper No. 2011-01-0390, 2011.
14. Jeon, C. H., Jeong, J. H., Kim, H. K., Song, J. H., and Chang, Y. J., "A Study on the Non-Evaporating Diesel Spray Characteristics as a Function of Ambient Pressure in Constant Volume Combustion Chamber," Journal of the Korean Society of Marine Engineering, Vol. 34, No. 5, pp. 645-652, 2010.
15. Ko, G. H., Ryou, H. S., Lee, S. H., and Hong, K. B., "Numerical Study on Drop Breakup in Air-Assisted Spray Using the TAB Model with a Modified Drop Drag Model," Transactions of Korean Society of Automotive Engineers, Vol. 10, No. 2, pp. 87-95, 2002.
16. Seo, Y. T., Suh, H. K., and Lee, C. S., "A Study on the Injection Characteristics of Biodiesel Fuels Injected through Common-rail Injection System," Transactions of the Korean Society of Automotive Engineers, Vol. 15, No. 5, pp. 97-104, 2007.